Engineering Structures 137 (2017) 145–161

Contents lists available at ScienceDirect

Engineering Structures

journal homepage: www.elsevier.com/locate/engstruct

Nonlinear finite-element analysis for the behavior prediction and strut efficiency factor of GFRP-reinforced concrete deep beams

Khaled Mohamed, Ahmed Sabry Farghaly, Brahim Benmokrane *, Kenneth W. Neale

Department of Civil Engineering, University of Sherbrooke, Sherbrooke, Quebec J1K 2R1, Canada

ARTICLE INFO

Article history:
Received 16 September 2016
Revised 22 December 2016
Accepted 19 January 2017
Available online 6 February 2017

Keywords:
Concrete
GFRP bars
Failure mechanisms
Deep beams
FEA
STM

ABSTRACT

The recent experimental results and proposed strut-and-tie model (STM) for deep beams reinforced entirely with glass-fiber-reinforced polymer (GFRP) bars have suggested that a comprehensive examination is required to improve the strut efficiency factor and its affecting parameters. This study uses nonlinear finite-element analysis (FEA) to perform an in-depth investigation. FEA response was compared against the experimental results in terms of crack patterns, failure modes, strains in reinforcement and concrete, and load–deflection relationships. The results show that the simulation procedures employed were stable and compliant, and that they provided reasonably accurate simulations of the behavior. FEA was used to confirm some hypotheses associated with the experimental investigations. A comprehensive parametric study was conducted to investigate the effect of web reinforcement and loading-plate size on the strut efficiency factor. It was shown that vertical web reinforcement has no clear effect on the strength, but it is required for crack control. On the other hand, horizontal web reinforcement should be accompanied with vertical reinforcement. Loading-plate size showed a clear effect on the deep-beam strength. Based on the numerical simulation results, a modification to a recently proposed STM is suggested. The modified STM was compared to available STMs in design codes and provisions, yielding better correlation with experimental results.

1. Introduction

Reinforced-concrete deep beams are used mainly for load transfer, such as transfer girders, bent caps, and pile caps. The behavior of reinforced-concrete deep beams is different from that of slender beams because of their relatively larger magnitude of shearing and normal stresses (Rueter [1]). Unlike slender beams, deep beams transfer shear forces to supports through compressive stresses rather than shear stresses. The diagonal cracks in deep beams eliminate the inclined principal tensile stresses required for beam action and lead to a redistribution of internal stresses, so that the beam acts as a tied arch (Slight [2]). These structural elements are subjected to deterioration due to the freeze–thaw cycles and the corrosion of steel bars resulting from the large amount of deicing salts used during winter months. Replacing steel bars with noncorrodible fiber-reinforced polymer (FRP) in reinforced-concrete elements has become an acceptable solution to overcome steel-corrosion problems. Experimental investigations on FRP-reinforced deep beams, however, have been very limited, particularly for those lacking web reinforcement (Andermatt and Lubell [3], Farghaly and Benmokrane [4], Kim et al. [5]).

Codes and provisions have adopted the use of strut-and-tie model (STM) for the design of steel-reinforced deep beams (ACI 318 [6], CSA A23.3 [7], *fib* [8], Eurocode2 [9]) and FRP-reinforced deep beams (CSA S806 [10]). The STM is applicable for deep beams as the plane section does not remain plane and nonlinear shearing strains dominate the behavior. Many researchers have developed simplified expressions to predict the capacity of deep beams based on the STM (Matamoros and Wong [11], Russo et al. [12], Park and Kuchma [13], Mihaylov et al. [14]). While the STM provides a simple design methodology based on the lower-bound theorem, its implementation requires an iterative process and graphical assumption for the truss model. The developed expressions are governed by the variables affecting the deep-beam behavior, such as concrete compressive strength, shear span–depth ratio, and the modulus of elasticity of the longitudinal and web reinforcement. The accuracy of the developed expressions is, however, affected by the estimated factor for each of these variables. Moreover, the factor of each variable is estimated based on the available experimental results, which could be limited in number, or insufficient analytical results that cannot be obtained from experiments.

* Corresponding author.
E-mail addresses: Khaled.Mohamed@USherbrooke.ca (K. Mohamed), Ahmed.Farghaly@USherbrooke.ca (A.S. Farghaly), Brahim.Benmokrane@USherbrooke.ca (B. Benmokrane), Kenneth.Neale@USherbrooke.ca (K.W. Neale).

http://dx.doi.org/10.1016/j.engstruct.2017.01.045
0141-0296/

Finite-element analysis (FEA) is considered as an alternative for in-depth analysis. FEA is currently the most complex and advanced approach for predicting the response of reinforced-concrete structures. Therefore, a parametric study was conducted to investigate other affecting variables such as the web reinforcement ratio and the loading-plate size.

2. Description of the GFRP-reinforced deep beams tested

Ten full-scale reinforced concrete deep beams with constant rectangular cross sections 1200 mm in height (h) and 300 mm in width (b) were constructed and tested to failure under two-point loading. The parameters of the experimental program were a/d (equal to 1.47, 1.13, and 0.83) and web-reinforcement configuration (vertical only, horizontal only, or vertical and horizontal web reinforcement), as presented in Table 1. Fig. 1a and b, respectively, show dimensions and details of the tested specimens and testing setup. A series of linear variable differential transducers (LVDTs) and/or strain gauges were used to measure the deflection, strains, and deformation of the tested specimens, as shown in Fig. 1c. The tested deep beams were reinforced with sand-coated GFRP bars of various diameters: #4 and #5 for the vertical and horizontal web reinforcement, respectively, and #8 for the main longitudinal reinforcement. Table 2 summarizes the mechanical properties of the GFRP bars as provided by the manufacturer (Pultrall Inc., Thetford Mines, Quebec [15]).

Fig. 2 shows the typical normalized load–deflection response for specimens with an a/d of 1.13. All the tested specimens exhibited a nearly bilinear response up to failure. The first crack to

Table 2
Reinforcement material properties.

Bar type	Bar diameter, φ_f[a] (mm)	Nominal cross-sectional area, A_{frp} (mm^2)	Ultimate tensile strength, f_{fu} (MPa)	Modulus of elasticity, E_{frp} (GPa)
Straight bars				
GFRP	15 (#5)	197.9	1184	62.6
	25 (#8)	506.7	1000	66.4
Steel	8 (#10)	50	f_y = 400	200
Bent bars				
GFRP	13 (#4)	126.7	1312	65.6

[a] Number between parentheses are the manufacturer's bar designation.

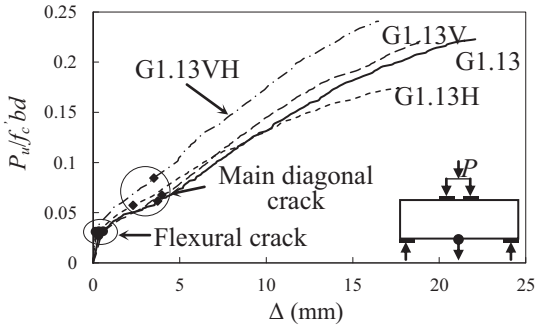

Fig. 2. Load–deflection response for specimens with a/d of 1.13.

Table 1
Details of the tested GFRP-reinforced deep beams.

Deep beam ID	f_c' (MPa)	a (mm)	Longitudinal reinforcement		Web reinforcement				Exp.		FEM		P_{exp}/P_{pred}
			A_{frp} (mm^2)	E_{frp} (GPa)	Vertical		Horizontal		P_{exp} (kN)	$P_{exp}/f_c'bd$	P_{pred} (kN)	$P_{pred}/f_c'bd$	
					S_v (mm)	ρ_v (%)	S_h (mm)	ρ_h (%)					
G1.47	38.7	1600	4054	66.4	–	–	–	–	1849	0.146	1761	0.139	1.05
G1.47H	45.4	1600	4054	66.4	–	–	195	0.66	1695	0.114	1591	0.107	1.07
G1.47V	45.4	1600	4054	66.4	200	0.42	–	–	2650	0.179	2325	0.157	1.14
G1.13	37	1250	4054	66.4	–	–	–	–	2687	0.223	2501	0.207	1.08
G1.13H	44.6	1250	4054	66.4	–	–	195	0.66	2533	0.174	2140	0.147	1.18
G1.13V	44.6	1250	4054	66.4	200	0.42	–	–	3236	0.222	2610	0.179	1.24
G1.13VH	37	1250	4054	66.4	200	0.42	195	0.66	2904	0.241	2400	0.199	1.21
G0.83	38.7	900	4054	66.4	–	–	–	–	3000	0.238	3125	0.247	0.96
G0.83H	43.6	900	4054	66.4	–	–	195	0.66	3166	0.223	3314	0.233	0.96
G0.83V	43.6	900	4054	66.4	200	0.42	–	–	3387	0.238	3456	0.242	0.98

Note: For all specimens, h = 1200 mm, d = 1088 mm, b = 300 mm; loading and support-plate widths: 203 and 232 mm, respectively. P_{exp} is the experimental capacity and P_{pred} is the predicted capacity. S and ρ are the web-reinforcement spacing and ratio, respectively. For specimens with web reinforcement, the diameters of vertical and horizontal web bars are 13 mm and 15 mm, respectively.

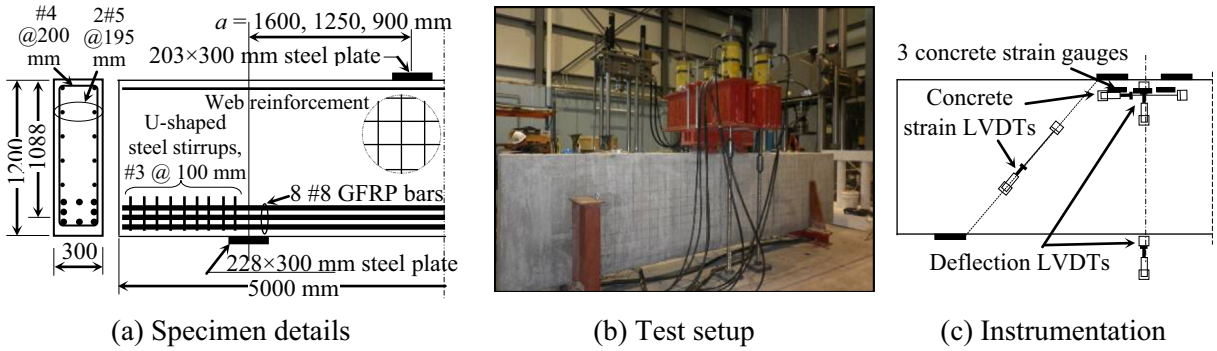

Fig. 1. Specimen details, test setup, and specimen instrumentation.